Proceedings of the Seventh International Conference on
Railway Technology: Research, Development and Maintenance
Edited by: J. Pombo
Civil-Comp Conferences, Volume 15, Paper 9.9
Civil-Comp Press, Edinburgh, United Kingdom, 2026
ISSN: 2753-3239, doi: 10.4203/ccc.15.9.9

Leading-Axle Active Probing of Wheel-Rail Adhesion under Low-Adhesion Braking Conditions

X. Wu[1,2], J. Zuo[1,2] and J. Ding[1,2]

[1]College of Transportation, Tongji University, Shanghai, China
[2]Shanghai Key Laboratory of Rail Infrastructure Durability and System Safety, Tongji University, China

Abstract

Wheel–rail adhesion uncertainty is a key challenge for railway braking control and wheel slide protection. This paper proposes a leading-axle active adhesion probing method to estimate the utilized adhesion coefficient at a prescribed slip-ratio threshold during braking. The leading axle is used as a probing wheelset because it first encounters the unknown rail surface ahead. A bounded brake-cylinder pressure excitation is applied to the leading axle, driving the wheel–rail operating point towards the target slip-ratio region while maintaining a safe small-slip condition. Meanwhile, the current utilized adhesion coefficient is estimated online using an unscented Kalman filter based on the coupled longitudinal–rotational dynamics of the wheelset. Instead of identifying a complete adhesion–slip curve, the proposed method records the estimated adhesion coefficient when the leading-axle slip ratio reaches the prescribed threshold. A SIMPACK multibody dynamics model of a four-car urban rail vehicle is established to validate the method under different speed levels and adhesion-transition scenarios. The simulation results indicate that the proposed logic can complete controlled pressure probing, update the utilized adhesion estimate, and limit excessive wheel slip risk.

Keywords: railway braking, wheel–rail adhesion, low adhesion, braking safety, leading-axle active probing, brake cylinder pressure control.

1 Introduction

Wheel–rail adhesion is fundamental to braking-force transmission in railway vehicles, and its utilization directly affects train deceleration, wheel-slide risk, and braking safety. It is commonly described by an adhesion–slip curve: the adhesion coefficient increases with slip ratio, reaches a peak near the critical slip region, and then decreases or becomes unstable as the wheelset enters sliding [1, 2]. Under low-adhesion conditions caused by rain, fallen leaves, snow, or ice, the available adhesion can decrease significantly. The demanded braking force may then exceed the current adhesion limit, causing wheel slide, extended braking distance, and frequent wheel-slide protection (WSP) actions [3, 4].

Current railway vehicles mainly rely on WSP systems to suppress wheel slide. When abnormal wheel-speed differences, slip ratios, or deceleration signals are detected, the brake-cylinder pressure is reduced to return the wheelset to a safe operating region [5, 6]. Although this reactive strategy ensures basic safety, it reduces braking force only after wheel slide has begun to develop. Under low adhesion, repeated pressure reduction and re-establishment may degrade braking-force continuity, reduce adhesion utilization, and increase braking distance. Therefore, obtaining wheel–rail adhesion information before severe wheel slide occurs is important for braking-force regulation and WSP optimization.

Wheel–rail adhesion estimation has been studied through braking tests, wheel-slide events, model-based estimation, observers, filtering algorithms, and data-driven methods. Event-based methods can infer adhesion near the onset of sliding, but the probing timing and slip-ratio level are not actively controllable [7–10]. Model-based and data-driven methods can estimate utilized adhesion near the current operating point [11], but they generally do not drive the wheel–rail operating point toward a specified slip-ratio threshold. Therefore, they are limited in providing adhesion information at a controlled slip level before severe wheel slide occurs.

To address this gap, this paper proposes a slip-threshold-based adhesion estimation method using leading-axle brake probing. The leading axle is selected because it is the first axle to encounter the unknown rail surface in the direction of travel, and its slip response provides the earliest indication of the adhesion condition ahead. In the proposed method, the leading-axle brake-cylinder pressure is controlled under safety constraints so that the wheel–rail operating point approaches a prescribed slip-ratio threshold. The real-time estimated utilized adhesion coefficient at that moment is taken as the adhesion level corresponding to the specified threshold. This information can support subsequent braking-force regulation, WSP parameter optimization, and coordination between regenerative and pneumatic braking.

2 Methods

2.1 Braking Slip Ratio and Adhesion Coefficient

Wheel–rail adhesion is commonly described by an adhesion coefficient–slip ratio characteristic curve, as illustrated in Figure 1. The horizontal axis represents the wheelset slip ratio, which reflects the relative difference between the wheel circumferential speed and the vehicle running speed. The vertical axis represents the adhesion coefficient, defined as the ratio of the longitudinal tangential wheel–rail force to the normal contact force. In a typical adhesion–slip relationship, the adhesion coefficient increases with slip ratio in the small-slip region and reaches a peak near a critical slip value. As the slip ratio continues to increase, the adhesion coefficient may become saturated or decrease. Rolling contact theory and wheel–rail creep force models have shown that the longitudinal wheel–rail force has a strongly nonlinear relationship with slip ratio.

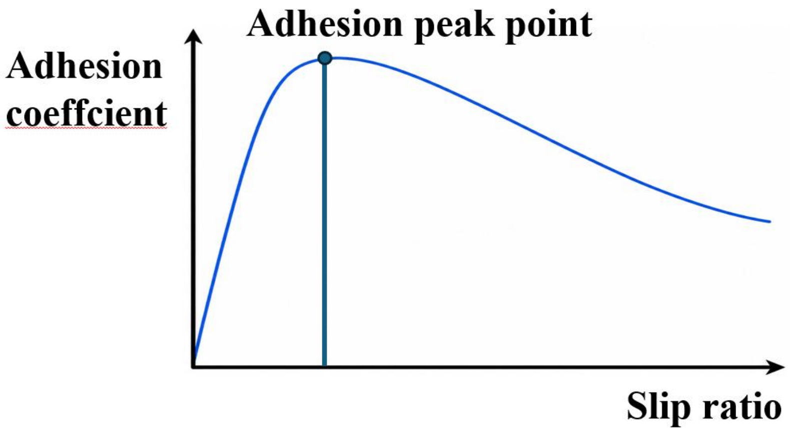

Figure 1: Wheel–rail adhesion characteristic curve.

The slip ratio on the horizontal axis is defined as the ratio of the difference between the vehicle reference speed and the wheel circumferential speed to the vehicle reference speed, namely,

$$\lambda = \frac{v - v_w}{v} = \frac{v - R\omega}{v} \tag{1}$$

where v is the vehicle reference speed, v_w is the wheel circumferential speed, R is the effective rolling radius of the wheel, and ω is the angular velocity of the wheelset. When $\lambda = 0$, the wheelset is approximately in a pure rolling condition. As λ increases, the wheelset exhibits a stronger tendency towards sliding. When the wheel approaches a locked condition, v_w tends to zero and λ approaches unity.

Correspondingly, the current adhesion coefficient can be defined as

$$\mu = \frac{|F_y|}{N} \tag{2}$$

where F_y is the magnitude of the longitudinal wheel–rail force, and N is the magnitude of the normal wheel–rail contact force. This definition represents the wheel–rail adhesion level utilized by the wheelset under the current braking condition.

It should be noted that the adhesion coefficient–slip ratio curve is not fixed. Rail surface conditions such as dry, wet, oil-contaminated and leaf-contaminated rails can change the adhesion peak, the initial slope and the corresponding peak slip ratio.

Braking tests have also shown that adhesion is affected by wheel slip state, train speed and artificially degraded adhesion conditions.

In practical braking, the rail surface ahead of the vehicle is uncertain and time-varying. Therefore, a single fixed adhesion curve may not accurately describe the actual wheel–rail adhesion state. To reduce this dependence, this study proposes a leading-axle active adhesion probing method, in which the slip response is actively regulated during braking to estimate the current wheel–rail adhesion in real time.

2.2 Overall Concept of the Leading-Axle Active Adhesion Probing Method

As illustrated in Figure 2, the proposed method combines controlled leading-axle brake-cylinder pressure excitation with online estimation of the current wheel–rail adhesion state. During braking, the controller regulates the leading-axle brake-cylinder pressure through the pneumatic brake circuit and actuator, so that the wheelset produces a measurable adhesion response within a safe small-slip region. Meanwhile, the adhesion estimation module continuously estimates the current adhesion coefficient from measurable signals, including wheelset rotational speed and brake-cylinder pressure. When the leading-axle slip ratio reaches a prescribed threshold during the controlled pressure increase, the corresponding estimated adhesion coefficient is recorded as the adhesion level at that threshold. Rather than identifying the complete adhesion–slip curve, this method focuses on obtaining threshold-specific adhesion information for brake force allocation and wheel slide protection control.

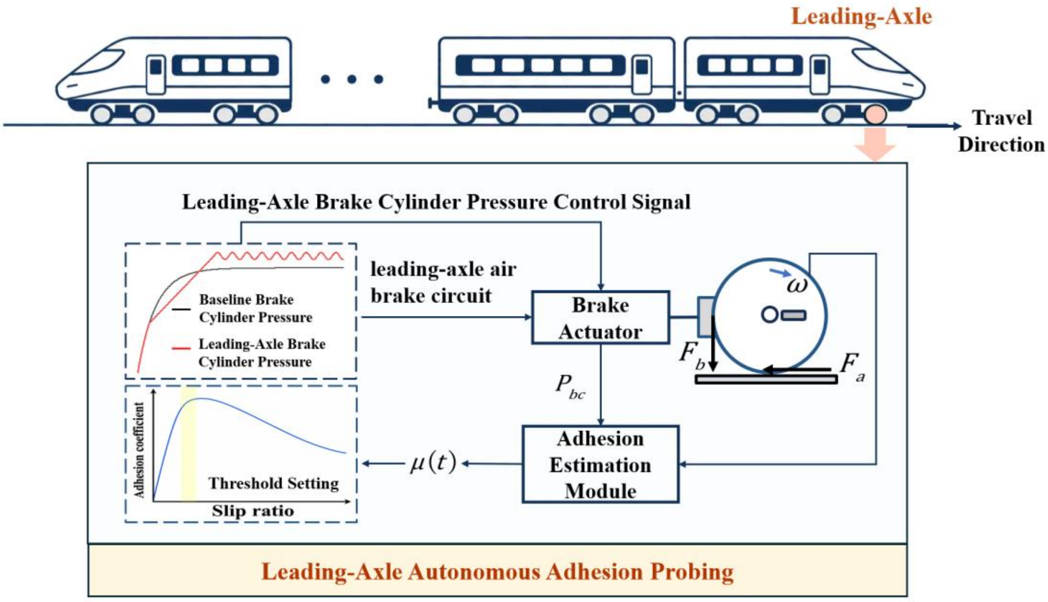

Figure 2: Overall framework of the leading-axle active adhesion probing method.

To avoid unintended intervention of the existing wheel slide protection system, the active probing function is enabled only when the probing command is valid, the vehicle speed is higher than the low-speed threshold, the braking command is active, and no wheel slide protection command is present. Once a wheel slide protection command, emergency braking command, actuator fault, or sensor fault is detected, the probing process is immediately terminated. Therefore, the proposed method is not intended to replace the conventional wheel slide protection system. Rather, it provides current adhesion information in advance through bounded pressure excitation before wheel slide protection intervention, thereby offering a reference for subsequent brake force allocation and wheel slide protection control.

2.3 Real-Time Estimation of Wheelset Utilized Adhesion

The current wheel–rail adhesion coefficient is estimated online using an unscented Kalman filter (UKF). The proposed method does not directly infer the adhesion coefficient by inverting the Polach adhesion curve. Instead, it first estimates the longitudinal creep force based on the coupled longitudinal–rotational dynamics of the wheelset, and then normalises the estimated creep force by the normal load to obtain the current adhesion coefficient. Therefore, the method is essentially a dynamics-based state-observation approach.

The state vector is defined as

$$\mathrm{x}_k = [v_k \quad \omega_k \quad F_{\gamma,k}]^{\mathrm{T}} \tag{3}$$

where v_k is the longitudinal velocity of the wheelset, $\omega_k$is the angular velocity of the wheelset, and $F_{\gamma,k}$ is the longitudinal creep force. The input is the braking torque $T_{\mathrm{br},k}$, and the measured output is the wheelset angular velocity z_k. The discrete-time system model is formulated as

$$v_{k+1} = v_k + \frac{T_s F_{\gamma,k}}{m} + w_{1,k} \tag{4}$$

$$\omega_{k+1} = \omega_k + \frac{T_s(R_w F_{\gamma,k} | T_{\mathrm{br},k})}{J} + w_{2,k} \tag{5}$$

$$F_{\gamma,k+1} = F_{\gamma,k} + w_{3,k} \tag{6}$$

$$z_k = \omega_k + \nu_k \tag{7}$$

where $m$is the single-axle equivalent mass, J is the rotational inertia of the wheelset, R_w is the wheel rolling radius, and T_s is the sampling period. The terms $w_{1,k}$, $w_{2,k}$, and $w_{3,k}$ denote process noise, while ν_k denotes measurement noise. In this formulation, the longitudinal creep force is treated as a random-walk state, so that variations in wheel–rail contact conditions and unmodelled disturbances can be represented in a compact form.

At each sampling instant, the UKF performs state prediction and measurement correction based on the above model, yielding the estimated longitudinal creep force $\hat{F}_{\gamma,k}$. The current longitudinal adhesion coefficient is then obtained by normalising this estimated force using the single-axle normal load,

$$F_N = m_{\mathrm{axle}} g \tag{8}$$

which gives

$$\hat{\alpha}_{x,k} = \frac{\hat{F}_{y,k}}{F_N} \tag{9}$$

where m_{axle} is the axle load mass and g is the gravitational acceleration.

Thus, the current adhesion coefficient defined in this study is essentially the ratio between the estimated longitudinal creep force and the normal wheel–rail contact load. This formulation is structurally clear and straightforward to implement. More importantly, it avoids the need for online identification of the parameters of a prescribed adhesion characteristic curve.

2.4 Leading-Axle Active Adhesion Probing Logic

To obtain the current wheel–rail adhesion state during braking, this study designs a safety-constrained active probing logic for the leading axle, as shown in Fig. 3. The probing function is enabled only under safe braking conditions, including a valid probing command, an active braking command, a vehicle speed above the prescribed threshold, and no WSP intervention. It is immediately terminated in the presence of WSP activation, emergency braking, or sensor/actuator faults. Therefore, the proposed method does not replace the existing WSP system but acts as an upper-level adhesion perception module before WSP intervention.

The proposed controller has two main features. The first feature is a three-stage pressure-increase strategy. Instead of applying a single continuous pressure ramp, the leading-axle brake-cylinder pressure is increased progressively through initial pressure build-up, staged pressure increase, and fine pressure probing. In the initial pressure build-up stage, a small, bounded pressure is applied to check the pressure response and preliminarily observe the slip behaviour. If the wheelset remains in a low-slip condition, the controller enters the staged pressure-increase stage, where the pressure is raised stepwise to further excite an observable slip response. Once the slip ratio or axle deceleration reaches the low threshold, the controller switches to the fine pressure-probing stage. In this stage, the pressure is increased at a lower rate so that the wheel–rail operating point approaches the prescribed slip-ratio threshold smoothly and safely. When the target slip-ratio threshold, high axle-deceleration threshold, or pressure limit is reached, the pressure increase is stopped, and the corresponding utilized adhesion estimate is recorded as the adhesion level at the specified slip threshold.

The second feature is a five-block operating structure. The controller is organized into five functional blocks: initial pressure build-up, staged pressure increase, fine pressure probing, pressure reduction and recovery, and rapid pressure reduction. The first three blocks from the main three-stage pressure-increase probing process, which is used to actively generate a measurable adhesion response within the safety boundary. The pressure reduction and recovery block is used after a valid probing response has been obtained; it reduces the brake-cylinder pressure until the slip ratio and axle deceleration return to the low-slip range, after which the controller can return to the staged pressure-increase block for repeated probing. The rapid pressure-reduction block is not a normal sequential stage, but a high-priority safety branch. It can be triggered from any operating block when the slip ratio exceeds the safety threshold, and the controller is allowed to return to staged pressure increase only after the slip response has recovered.

Overall, the logic achieves active adhesion probing through a controlled three-stage pressure increase, while maintaining braking safety through recovery and rapid pressure-reduction branches. This structure enables the leading axle to approach the specified slip-ratio threshold in a bounded manner, thereby providing current adhesion information for subsequent brake-force regulation and WSP parameter optimization.

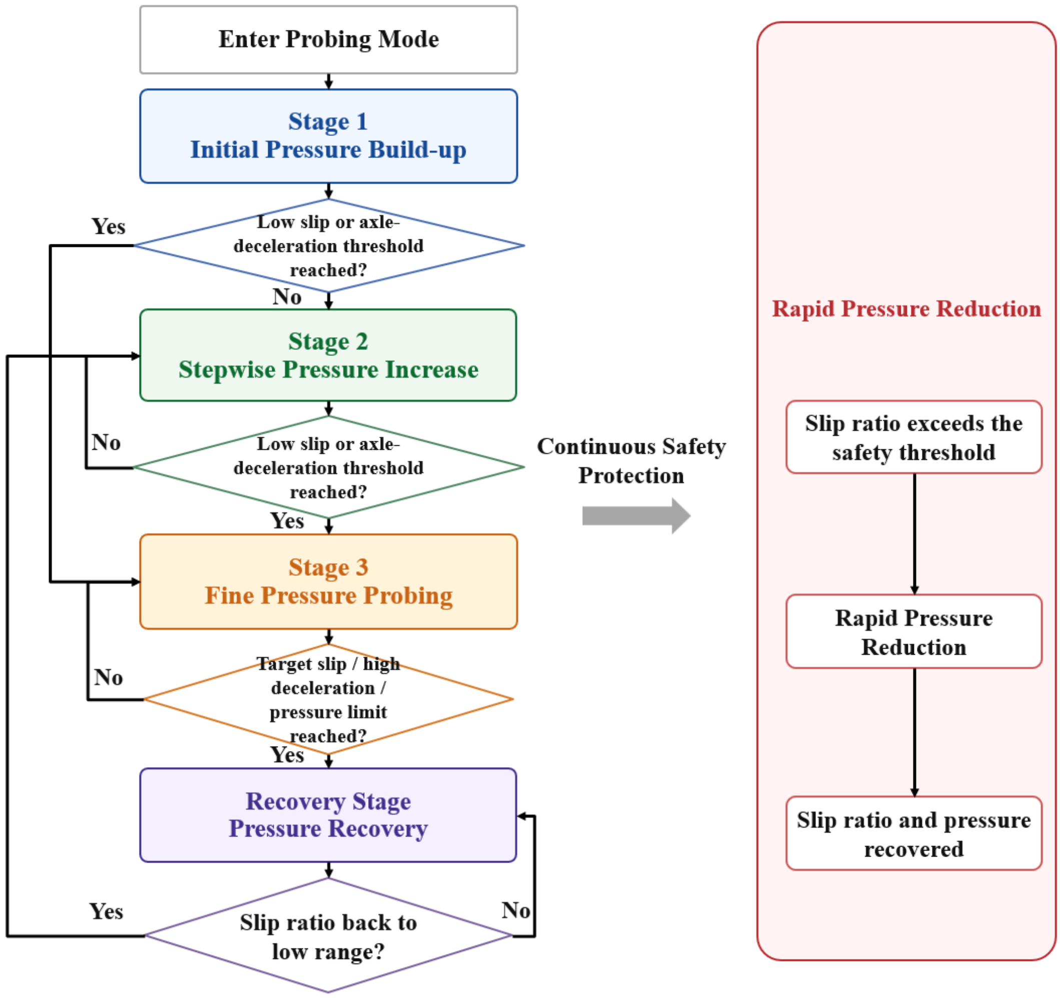

Figure 3: Leading-axle active adhesion probing logic.

3 Results

To verify the feasibility of the proposed leading-axle active braking probing method, a multibody dynamics model of a four-car urban rail vehicle was established in SIMPACK, as shown in Figure 4. The model simulates the vehicle longitudinal dynamics, wheel–rail contact, wheelset rotational response and brake-cylinder pressure variation during braking.

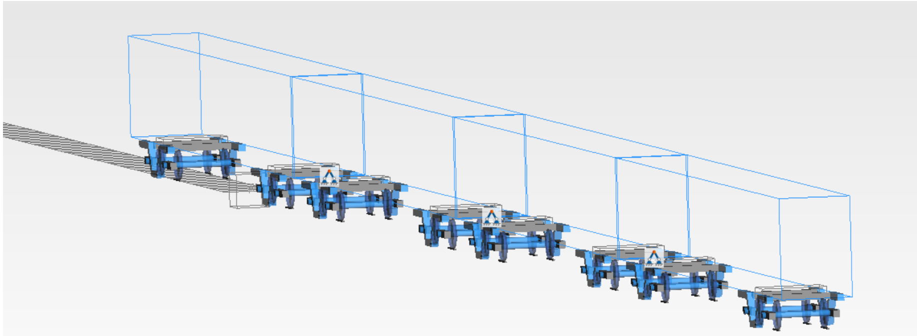

Figure 4: SIMPACK multibody dynamics model of the four-car urban rail vehicle.

In the simulation, the leading axle follows the proposed active probing logic, while the remaining wheelsets apply the baseline braking command. The leading-axle angular velocity, vehicle reference speed and brake-cylinder pressure are recorded to calculate the slip ratio, estimate the current utilized adhesion coefficient and evaluate the safety constraints.

To verify the effectiveness and applicability of the proposed leading-axle wheel–rail adhesion probing method under different operating conditions, this study considers both the initial braking speed and variations in rail adhesion. Three typical braking cases are designed, corresponding to low-, medium-, and high-speed conditions. To highlight the capability of low-adhesion identification and response to adhesion transitions, each speed case adopts a track adhesion profile composed of sequential high-, medium-, and low-adhesion sections. This setting represents the practical situation in which a train passes through rail sections with different surface conditions during braking. The designed cases enable the dynamic response of the leading-axle probing logic to be evaluated at different speeds, while also assessing its real-time perception capability and safety constraints under abrupt adhesion changes.

The specific simulation cases are listed in Table 1. The simulation results are presented in Figs. 5, 6, and 7, respectively, showing the time-domain responses of the leading-axle brake-cylinder pressure, slip ratio, probing state, and current adhesion estimation results under different speed conditions. By comparing whether the leading-axle slip ratio approaches the prescribed threshold within the safe range, whether the brake-cylinder pressure follows the staged probing logic, whether the estimated adhesion varies consistently with the high-, medium-, and low-adhesion sections, and whether excessive slip or WSP activation occurs, the probing performance and engineering feasibility of the proposed method are evaluated.

Initial braking speed [km/h]	High adhesion $\mu = 0.3$	Low adhesion $\mu = 0.1$	Very low adhesion $\mu = 0.06$
30	0-22 m	22-44 m	> 44 m
60	0-66 m	66-132 m	>132 m
90	0-144 m	144-288m	>288 m

Table 2: Simulation scenario design.

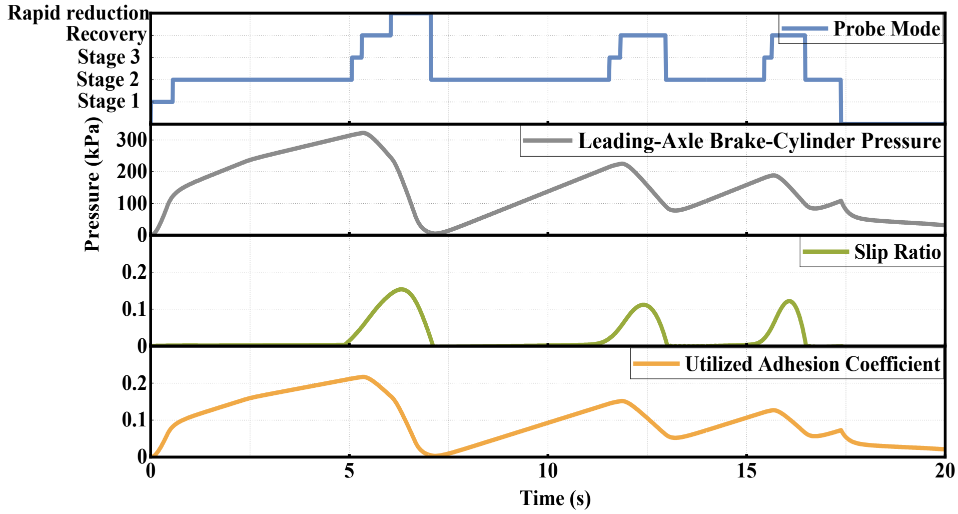

Figure 5: Time-domain response of leading-axle active adhesion probing at 30 km/h.

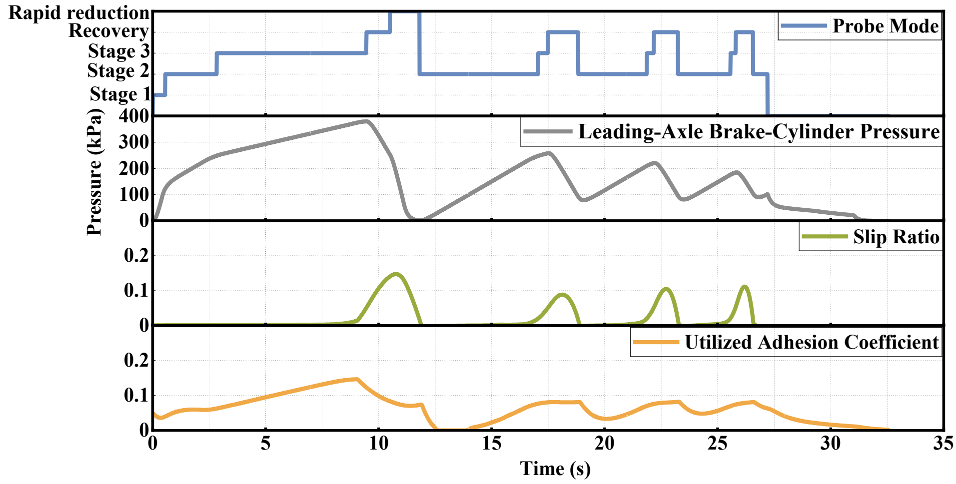

Figure 6: Time-domain response of leading-axle active adhesion probing at 60 km/h.

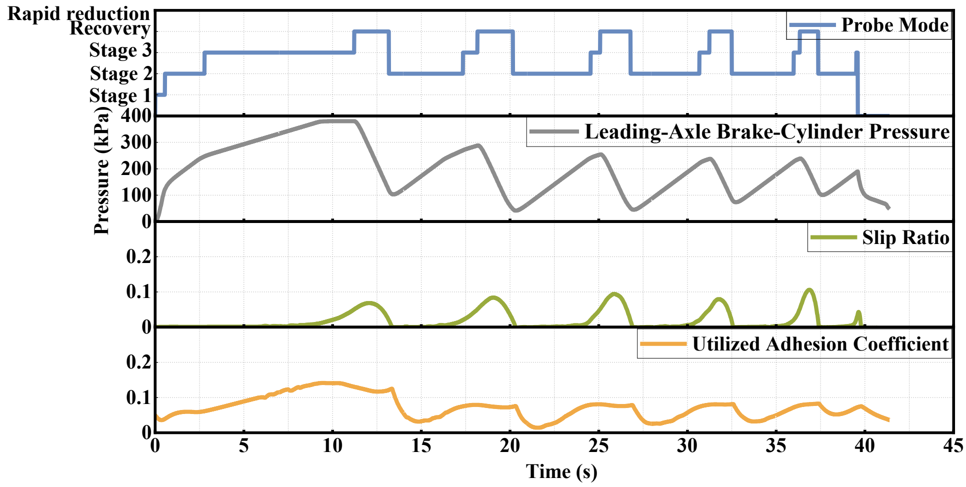

Figure 7: Time-domain response of leading-axle active adhesion probing at 90 km/h.

It can be observed that, in the 30, 60, and 90 km/h cases, the controller switches among the initial pressure build-up, staged pressure increase, fine pressure probing, and pressure recovery states according to the predefined logic. The leading-axle brake-cylinder pressure is progressively increased to excite a measurable slip response. When the slip ratio approaches the prescribed threshold or shows a rapid increasing tendency, the controller stops the pressure increase in time and enters the pressure recovery or rapid pressure-reduction process, so that the slip ratio returns to the low-slip range. This indicates that the probing process can operate within the safety boundary.

As the train passes through the connected high-, medium-, and low-adhesion sections, the utilized adhesion coefficient of the leading axle changes accordingly. In the high-adhesion section, the brake-cylinder pressure can rise to a relatively high level, and the estimated adhesion coefficient is also higher. After entering the medium- and low-adhesion sections, a more pronounced slip response is generated under the same or even lower pressure level, and the utilized adhesion coefficient decreases correspondingly.

Comparing the three speed cases, the probing duration becomes longer and the number of pressure probing–recovery cycles increases as the initial speed increases. Nevertheless, the slip ratio remains constrained within a controllable range, demonstrating the applicability of the proposed method under different speeds and adhesion-transition conditions.

Overall, the results show that leading-axle brake-pressure probing can effectively drive the wheel–rail operating point toward the target slip region and reflect changes in the current rail adhesion level in real time, thereby providing prior adhesion information for subsequent braking-force regulation and WSP parameter optimization.

4 Conclusions and Contributions

This paper proposes a leading-axle active adhesion probing method for trains. By regulating the leading-axle brake-cylinder pressure within bounded limits, the proposed method drives the leading-axle slip ratio towards a prescribed threshold and estimates the current utilized adhesion coefficient in real time based on the coupled longitudinal–rotational dynamics of the wheelset. The main conclusions and contributions are as follows.

First, a leading-axle active adhesion probing framework for braking control is proposed. The framework exploits the fact that the leading axle is the first to encounter the unknown rail surface ahead. By applying a small and bounded brake pressure excitation, the leading axle can generate a measurable response within a safe slip range. This enables the acquisition of prior adhesion information before the intervention of the Wheel Slide Protection (WSP) system, thereby providing a basis for subsequent brake-force regulation.

Second, a real-time estimation method for the current utilized adhesion coefficient of the wheelset is established. The proposed method does not rely on a predefined complete adhesion coefficient–slip ratio curve. Instead, the longitudinal wheel–rail creep force is estimated and then normalised by the normal load to obtain the current utilized adhesion coefficient. When the leading-axle slip ratio reaches the prescribed threshold, the estimated value at that instant is taken as the adhesion level corresponding to that slip-ratio threshold, providing real-time information for adhesion-state assessment during braking.

Third, the active probing logic is validated through simulation. A state-based control logic including initial pressure build-up, stepwise pressure increase, fine pressure probing, pressure reduction and recovery, and safety release is designed. SIMPACK multibody dynamics simulations show that the proposed logic can execute the controlled pressure probing process in the tested scenarios. The results also indicate that the threshold-specific adhesion estimate can be obtained while excessive wheel slip is limited, demonstrating the effectiveness of the proposed logic in the simulation study.

Future work will further validate the adhesion estimation accuracy through brake rig tests or field tests. The integration of the proposed method with multi-axle brake-force allocation, adaptive adjustment of WSP parameters and other braking-control functions will also be investigated.

Acknowledgements

This work was supported by the National Key Research and Development Program of China (2024YFB4303300), Science and Technology Research and Development Programme Topics of China State Railway Group Co., Ltd. (P2023J040-4), and Shanghai Collaborative Innovation Research Center for Multi-network & Multi-model Rail Transit. The corresponding author of this paper is Prof. Jianyong Zuo.

References

[1] J. J. Kalker, Three-Dimensional Elastic Bodies in Rolling Contact. Dordrecht: Kluwer Academic Publishers, 1990.

[2] O. Polach, "Creep forces in simulations of traction vehicles running on adhesion limit," Wear, vol. 258, no. 7–8, pp. 992–1000, 2005.

[3] K. Ishizaka, S. R. Lewis, and R. Lewis, "The low adhesion problem due to leaf contamination in the wheel/rail contact: bonding and low adhesion mechanisms," Wear, vol. 378–379, pp. 183–197, 2017.

[4] Transit Cooperative Research Program, "Improved Methods for Increasing Wheel/Rail Adhesion in the Presence of Natural Contaminants," TCRP Research Results Digest, no. 17, Transportation Research Board, 1997.

[5] EN 15595:2018+A1:2023, Railway applications — Braking — Wheel slide protection. European Committee for Standardization, 2023.

[6] S. Nakazawa, "Development of a New Wheel Slide Protection System Using a New Detection Algorithm," Quarterly Report of RTRI, vol. 52, no. 3, pp. 136–140, 2011.

[7] EN 15595:2018+A1:2023, Railway applications — Braking — Wheel slide protection.
[8] CEN/TR 17315:2019, Railway applications — Braking — Calculations for the estimation of stopping distance for specific Wheel Slide Protection testing.
[9] M. Malvezzi, L. Pugi, S. Papini, A. Rindi, and P. Toni, "Identification of a wheel–rail adhesion coefficient from experimental data during braking tests," Proceedings of the Institution of Mechanical Engineers, Part F: Journal of Rail and Rapid Transit, vol. 227, no. 2, pp. 128–139, 2013.
[10] US7064507B2, "Managing wheel skid in a locomotive," 2006.
[11] S. Shrestha, Q. Wu, and M. Spiryagin, "Review of adhesion estimation approaches for rail vehicles," International Journal of Rail Transportation, vol. 7, no. 2, pp. 79–102, 2019.